J|A|C|S
ARTICLES
Published on Web 01/12/2006

# Tuning the Reactivity of Osmium(II) and Ruthenium(II) Arene Complexes under Physiological Conditions

Anna F. A. Peacock,[†] Abraha Habtemariam,[†] Rafael Fernández,[†] Victoria Walland,[†] Francesca P. A. Fabbiani,[†] Simon Parsons,[†] Rhona E. Aird,[‡] Duncan I. Jodrell,[‡] and Peter J. Sadler*[,†]

*Contribution from the School of Chemistry, University of Edinburgh, West Mains Road, Edinburgh EH9 3JJ, U.K., and Cancer Research UK Edinburgh Oncology Unit, University of Edinburgh Cancer Research Centre, Edinburgh EH4 2XR, U.K.*

Received September 13, 2005; E-mail: P.J.Sadler@ed.ac.uk

***Abstract:*** The $Os^{II}$ arene ethylenediamine (en) complexes [($\eta^6$-biphenyl)Os(en)Cl][Z], Z = $BPh_4$ (**4**) and $BF_4$ (**5**), are inactive toward A2780 ovarian cancer cells despite **4** being isostructural with an active $Ru^{II}$ analogue, **4R**. Hydrolysis of **5** occurred 40 times more slowly than **4R**. The aqua adduct **5A** has a low p$K_a$ (6.3) compared to that of [($\eta^6$-biphenyl)Ru(en)$(OH_2)$]$^{2+}$ (7.7) and is therefore largely in the hydroxo form at physiological pH. The rate and extent of reaction of **5** with 9-ethylguanine were also less than those of **4R**. We replaced the neutral en ligand by anionic acetylacetonate (acac). The complexes [($\eta^6$-arene)Os(acac)Cl], arene = biphenyl (**6**), benzene (**7**), and *p*-cymene (**8**), adopt piano-stool structures similar to those of the $Ru^{II}$ analogues and form weak dimers through intermolecular (arene)C−H···O(acac) H-bonds. Remarkably, these $Os^{II}$ acac complexes undergo rapid hydrolysis to produce not only the aqua adduct, [($\eta^6$-arene)Os(acac)$(OH_2)$]$^+$, but also the hydroxo-bridged dimer, [($\eta^6$-arene)Os($\mu^2$-OH)$_3$Os($\eta^6$-arene)]$^+$. The p$K_a$ values for the aqua adducts **6A**, **7A**, and **8A** (7.1, 7.3, and 7.6, respectively) are lower than that for [($\eta^6$-*p*-cymene)Ru(acac)$(OH_2)$]$^+$ (9.4). Complex **8A** rapidly forms adducts with 9-ethylguanine and adenosine, but not with cytidine or thymidine. Despite their reactivity toward nucleobases, complexes **6**−**8** were inactive toward A549 lung cancer cells. This is attributable to rapid hydrolysis and formation of unreactive hydroxo-bridged dimers which, surprisingly, were the only species present in aqueous solution at biologically relevant concentrations. Hence, the choice of chelating ligand in $Os^{II}$ (and $Ru^{II}$) arene complexes can have a dramatic effect on hydrolysis behavior and nucleobase binding and provides a means of tuning the reactivity and the potential for discovery of anticancer complexes.

## Introduction

The serendipitous discovery of the anticancer activity of cisplatin over 40 years ago[1] has stimulated the quest for other metal-based anticancer agents, especially complexes with fewer side effects than cisplatin, which circumvent developed and intrinsic resistance, and which possess a wider range of anticancer activity. Ruthenium(III) exhibits a spectrum of kinetic activity similar to that of $Pt^{II}$,[2] and two $Ru^{III}$ complexes have entered clinical trials, *trans*-[$RuCl_4$(DMSO)(Im)]ImH (NAMI-A, where Im = imidazole)[3] and *trans*-[$RuCl_4(Ind)_2$]IndH (KP1019, where Ind = indazole).[4] It has been proposed that their mode of action involves in vivo reduction of $Ru^{III}$ to the more reactive $Ru^{II}$.[2,5] Organometallic complexes offer a broad scope for the design of therapeutic and diagnostic agents.[6] Certain $Ru^{II}$ arene complexes of the type [($\eta^6$-arene)Ru(LL)(X)][Z] (where LL is a chelating ligand such as ethylenediamine (en), X a leaving group such as $Cl^-$, and Z a counterion) exhibit both in vitro and in vivo activity, in some cases with activity comparable to that of cisplatin and carboplatin.[7,8] Structure−activity relationships for these monofunctional $Ru^{II}$ complexes with respect to the arene,[8] the chelating ligand[9] (LL), and the leaving group[10] (X) have been studied. Some related acetylacetonate (acac) complexes [($\eta^6$-arene)Ru(acac)(Cl)] are also cytotoxic to cancer cells.[11] As for cisplatin, hydrolysis (substitu-

[†] School of Chemistry, University of Edinburgh.
[‡] Cancer Research UK Edinburgh Oncology Unit.

(1) Rosenberg, B.; VanCamp, L.; Trosko, J. E.; Mansour, V. H. *Nature* **1969**, 222, 385−386.
(2) Clarke, M. J.; Zhu, F.; Frasca, D. R. *Chem. Rev.* **1999**, *99*, 2511−2533.
(3) Sava, G.; Alessio, E.; Bergamo, A.; Mestroni, G. In *Topics in Biological Inorganic Chemistry*; Clarke, M. J., Sadler, P. J., Eds.; Springer-Verlag: Berlin, 1999; Vol. 1, pp 143−169.
(4) Galanski, M.; Arion, V. B.; Jakupec, M. A.; Keppler, B. K. *Curr. Pharm. Des.* **2003**, *9*, 2078−2089.
(5) Clarke, M. J.; Bitler, S.; Rennert, D.; Buchbinder, M.; Kelman, A. D. *J. Inorg. Biochem.* **1980**, *12*, 79−87.
(6) (a) Fish, R. H.; Jaouen, G *Organometallics* **2003**, *22*, 2166−2177. (b) Melchart, M.; Sadler, P. J. In *Bioorganometallics*; Jaouen, G., Ed.; Wiley-VCH: Paris; 2005; Vol. 1, pp 39−64. (c) Yan, Y. K.; Melchart, M.; Habtemariam, A.; Sadler, P. J. *Chem. Commun.* **2005**, 4764−4776.
(7) Aird, R. E.; Cummings, J.; Ritchie, A. A.; Muir, M.; Morris, R. E.; Chen, H.; Sadler, P. J.; Jodrell, D. I. *Br. J. Cancer* **2002**, *86*, 1652−1657.
(8) Morris, R. E.; Aird, R. E.; Murdoch, P. d. S.; Chen, H.; Cummings, J.; Hughes, N. D.; Parsons, S.; Parkin, A.; Boyd, G.; Jodrell, D. I.; Sadler, P. J. *J. Med. Chem.* **2001**, *44*, 3616−3621.
(9) Fernández, R.; Melchart, M.; Habtemariam, A.; Parsons, S.; Sadler, P. J. *Chem. Eur. J.* **2004**, *10*, 5173−5179.
(10) Wang, F.; Habtemariam, A.; van der Geer, E. P. L.; Fernández, R.; Melchart, M.; Deeth, R. J.; Aird, R.; Guichard, S.; Fabbiani, F. P. A.; Lozano-Casal, P.; Oswald, I. D. H.; Jodrell, D. I.; Parsons, S.; Sadler, P. J. *Proc. Natl. Acad. Sci. U.S.A.* **2005**, *102*, 18269−18274.
(11) Sadler, P. J.; et al. Unpublished results

tion of X by $H_2O$) may be an important step in the mechanism of action of $Ru^{II}$ arene complexes[12] and the rate-determining step in DNA binding. Here we explore the chemical and biological activity of arene en and acac complexes of the heavier congener $Os^{II}$. Previous reports on the aqueous chemistry of osmium arene complexes are limited.[13−15] Studies of the biological activity of osmium complexes appear to have been largely restricted to osmium carbohydrate polymers which exhibit antiarthritic activity.[16] Third-row transition metal ions are commonly more inert than those of the first and second rows. For example, substitution reactions of $Pt^{II}$ complexes are commonly ca. 5 orders of magnitude slower[17a] than those of its lighter congener $Pd^{II}$, and similarly $Os^{II}$ is generally found to be much more inert than its lighter congener $Ru^{II}$.[17] Here we show that the choice of the chelating ligand (LL = en or acac) in $[(\eta^6\text{-arene})Os(LL)Cl]^{n+}$ complexes can have a dramatic effect on hydrolysis behavior and reactivity toward nucleobases,[18] factors which are likely to be important in the design of $Os^{II}$ arene anticancer complexes.

## Experimental Section

**Materials.** 9-Ethylguanine, adenosine, cytidine, thymidine, and ethylenediamine were purchased from Sigma-Aldrich; deuterated solvents, ammonium tetraphenylborate, and ammonium tetrafluoroborate from Aldrich; and $OsCl_3 \cdot nH_2O$ from Alfa Aesar. Ethylenediamine was distilled over sodium; sodium acetylacetonate monohydrate was dried in vacuo; and ethanol and methanol were distilled over magnesium/iodine prior to use.

Complexes **1**−**8** were synthesized using procedures similar to those reported previously,[8,9] and the details and characterization of the complexes are given in the Supporting Information. Crystals suitable for X-ray diffraction were obtained at 253 K for **4** (from a saturated solution in acetone), **6**·0.25$CH_3OH$ (from THF/hexane solution), and **8** (by slow evaporation from an acetone/hexane solution) or at ambient temperature for **4R** (by diffusion of diethyl ether into a dichloromethane solution) and **7** (by the slow diffusion of diethyl ether into a chloroform solution).

**Methods and Instrumentation. (a) X-ray Crystallography.** All diffraction data were collected using a Bruker (Siemens) Smart Apex CCD diffractometer equipped with an Oxford Cryosystems low-temperature device operating at 150 K. Absorption corrections for all data sets were performed with the multiscan procedure SADABS.[19] Structures were solved using either Patterson or direct methods (SHELXL[20] or DIRDIF[21]). Complexes were refined against $F$ or $F^2$ using SHELXTL, and H-atoms were placed in geometrically calculated positions. X-ray crystallographic data for complexes **4**, **4R**, **6**·0.25$CH_3OH$, **7**, and **8** are available as Supporting Information and have been deposited in the Cambridge Crystallographic Data Centre under the accession numbers CCDC 291587, 291588, 291589, 291590, and 291591, respectively.

**(b) NMR Spectroscopy.** $^1$H NMR spectra were acquired on Bruker DMX 500 ($^1$H = 500 MHz), AVA 600 ($^1$H = 600 MHz), or AVA 800 ($^1$H = 800 MHz) spectrometers using TBI [$^1$H, $^{13}$C, X] probe-heads equipped with $z$-field gradients. $^1$H NMR spectra in $D_2O$ were typically acquired with water suppression by Shaka's method[22] or with presaturation. $^1$H NMR chemical shifts were internally referenced to 1,4-dioxane (3.75 ppm) for aqueous solutions, ($CHD_2$)($CD_3$)SO (2.50 ppm) for DMSO-$d_6$, and $CHCl_3$ (7.26 ppm) for chloroform-$d$ solutions. All data processing was carried out using XWIN-NMR version 2.0 (Bruker U.K. Ltd.).

**(c) Mass Spectrometry.** Electrospray ionization mass spectra (ESI-MS) were obtained on a Micromass Platform II mass spectrometer, and $D_2O/H_2O$ solutions were infused directly. The capillary voltage was 3.5 V, and the cone voltage was varied between 10 and 45 V, depending on sensitivity. The source temperature was 353 K. Mass spectra were recorded with a scan range $m/z$ 200−1200 for positive ions.

**(d) pH* Measurement.** The pH* (pH meter reading without correction for effects of D on the glass electrode) values of NMR samples in $D_2O$ were measured at ca. 298 K directly in the NMR tube, before and after recording NMR spectra, using a Corning 240 pH meter equipped with an Aldrich micro combination electrode calibrated with Aldrich buffer solutions at pH 4, 7, and 10.

**(e) Hydrolysis.** A solution of **5** in 5% MeOD-$d_4$/95% $D_2O$ (v/v) (ca. 1 mM and 298 K) was prepared by dissolution of **5** in MeOD-$d_4$, followed by rapid dilution with $D_2O$, and $^1$H NMR spectra were recorded at various time intervals. The rate of hydrolysis was determined by fitting the data for concentrations (determined by $^1$H NMR peak integrals) versus time using the appropriate equation for pseudo-first-order kinetics using the program ORIGIN version 5.0 (Microcal Software Ltd.). Solutions of **6**, **7**, and **8** at ca. 2 mM concentrations were made up at 298 K in $D_2O$. Sonication (ca. 10 min) was employed to assist dissolution, and $^1$H NMR spectra were recorded at various time intervals. $^1$H NMR spectra were also recorded for solutions of **5**−**8** in $D_2O$ after addition of 1 mol equiv of $AgNO_3$ and removal of the AgCl precipitate by filtration through a glass wool plug, and after addition of excess NaCl (to give 0.15 M) to an equilibrium solution of **8** in $D_2O$. The $^1$H NMR spectrum of **8** after dissolution in a 1 M solution of NaCl in $D_2O$ was also recorded.

To mimic typical biological test conditions (concentrations and solvents), a 50 $\mu$M stock solution of **8** in 0.125% DMSO-$d_6$/99.875% $D_2O$ (v/v) (measured pH* 7.74) was prepared by dissolution of **8** in DMSO-$d_6$, followed by rapid dilution with $D_2O$. An aliquot of this stock solution was then diluted with $D_2O$ to give a 2 $\mu$M Os solution (measured pH* 8.27). The 800 MHz $^1$H NMR spectra were recorded after ca. 30 min at 298 K. Samples were then incubated at 310 K for 24 h (a typical cell exposure time and temperature) and $^1$H NMR spectra recorded at 310 K.

The pH* of a solution of **8** (ca. 2 mM) in $D_2O$ was adjusted from 2.1 to 10.2, and then reversed to 2.5 and retitrated to 11.8, by the addition of DCl or NaOH, and $^1$H NMR spectra were recorded.

**(f) Calculation of p$K_a$* Values.** For determinations of p$K_a$* values (p$K_a$ values determined for $D_2O$ solutions), the pH* values of solutions


(12) Wang, F.; Chen, H.; Parsons, S.; Oswald, I. D. H.; Davidson, J. E.; Sadler, P. J. *Chem. Eur. J.* **2003**, *9*, 5810−5820.
(13) Hung, Y.; Kung, W.; Taube, H. *Inorg. Chem.* **1981**, *20*, 457−463.
(14) Stebler-Röthlisberger, M.; Hummel, W.; Pittet, P. A.; Bürgi, H. B.; Ludi, A.; Merbach, A. E. *Inorg. Chem.* **1988**, *27*, 1358−1363.
(15) Mui, H. D.; Brumaghim, J. L.; Gross, C. L.; Girolami, G. S. *Organometallics* **1999**, *18*, 3264−3272.
(16) Hinckley, C. C.; Bemiller, J. N.; Strack, L. E.; Russell, L. D. *ACS Symp. Ser.* **1983**, *209*, 421−37.
(17) (a) Tobe, M. L.; Burgess, J. *Inorganic Reaction Mechanisms*; Addison-Wesley Longman Inc.: Essex, 1999. (b) Shriver, D. F.; Atkins, P. W. *Inorganic Chemistry*, 3rd ed.; Oxford University Press: Oxford, 1999; p 245. (c) Lay, P. A.; Harman, W. D. *Adv. Inorg. Chem.* **1991**, *37*, 219−379. (d) Richens, D. T. *The Chemistry of Aqua Ions*; Wiley: Chichester, 1997; pp 421−429. (e) Griffith, W. P. In *Comprehensive Coordination Chemistry*; Wilkinson, G., Ed.; Pergamon: Oxford, 1987; Vol. 4, Ch. 46, pp 519−633. (f) Ashby, M. T.; Alguindigue, S. S.; Khan, M. A. *Organometallics* **2000**, *19*, 547−552. (g) George, R.; Andersen, J. M.; Moss, J. R. *J. Organomet. Chem.* **1995**, *505*, 131−133. (h) Halpern, J.; Cai, L.; Desrosiers, P. J.; Lin, Z. *J. Chem Soc., Dalton Trans.* **1991**, 717−723.
(18) Peacock, A. F. A.; Fernández, R.; Walland, V.; Habtemariam, A.; Fabbiani, F. P. A.; Parsons, S.; Aird, R.; Jodrell, D. I.; Sadler, P. J. *Second International Symposium on Bioorganometallic Chemistry* (ISBOMC'04), University of Zürich: Zürich, Switzerland, 2004; abstract p 98.
(19) *SADABS: Area-Detector Absorption Correction*; Siemens Industrial Automation, Inc.: Madison, WI, 1996.
(20) Sheldrick, G. M. *SHELXL-97*, Program for the refinement of crystal structures; University of Gottingen: Gottingen, Federal Republic of Germany, 1997.
(21) Beurskens, P. T.; Beurskens, G.; Bosman, W. P.; de Gelder, R.; Garcia-Granda, S.; Gould, R. O.; Israel, R.; Smits, J. M. M. *DIRDIF*; Crystallography Laboratory, University of Nijmegen: Nijmegen, The Netherlands, 1996.
(22) Hwang, T. L.; Shaka, A. J. *J. Magn. Reson.* **1995**, *A112*, 275−279.

of **5A**, **6A**, **7A**, and **8A** in $D_2O$ (formed in situ by dissolution of the parent chloro complexes **5**−**8**) were varied from ca. 2.5 to ca. 10 by the addition of dilute NaOH, and $^1$H NMR spectra were recorded.

The pH titration curves were fitted to the Henderson−Hasselbalch equation using the program KALEIDAGRAPH,[23] with the assumption that the observed chemical shifts are weighted averages according to the populations of the protonated and deprotonated species. The errors in p$K_a$* values are estimated to be ca. ±0.04 unit. These p$K_a$* values can be converted to p$K_a$ values by use of the equation p$K_a$ = 0.929p$K_a$* + 0.42, suggested by Krezel and Bal,[24] for comparison with related values in the literature.

**(g) Interactions with Nucleobases.** The reaction of complex **5** or **8** with nucleobases typically involved the addition of a solution containing 1 mol equiv of nucleobase in $D_2O$ to an equilibrium solution of **5** or **8** in $D_2O$ (which contains largely aqua **5A** and chloro **5**, or largely aqua **8A** and hydroxo-bridged dimer **8B** complexes, respectively), or to a solution of **5A** (prepared by the addition of 1 mol equiv of $AgNO_3$ to a solution of **5** and removal of AgCl by filtration). The pH* value of the sample was adjusted if necessary with dilute NaOH so as to remain within a physiologically relevant range (close to 7). $^1$H NMR spectra of these solutions were recorded at 298 K at various time intervals.

A pH* titration of a solution containing equimolar **8** and 9-ethylguanine (9-EtG) was carried out from pH* 2 to 9, and $^1$H NMR spectra were recorded at 298 K. A solution containing **8** and equimolar adenosine (Ado) was also titrated at 298 K from pH* 7 to 1 by the addition of dilute $HClO_4$. For both titrations, the purine H8 chemical shifts (together with that for H2 of Ado) were plotted against pH* and the data fitted to the Henderson−Hasselbalch equation.

**(h) Cytotoxicity toward A2780 and A549 Human Cancer Cells.** After plating, human ovarian A2780 cancer cells were treated with Os$^{II}$ complexes on day 3, and human lung A549 cancer cells on day 2, at concentrations ranging from 2 to 50 $\mu$M. Solutions of the Os$^{II}$ complexes were made up in 0.125% DMSO to assist dissolution. Cells were exposed to the complexes for 24 h, washed, supplied with fresh medium, and allowed to grow for three doubling times (72 h), and then the protein content was measured (proportional to cell survival) using the sulforhodamine B (SRB) assay.[25]

## Results

The complexes studied in this work are shown in Chart 1. Osmium(II) arene complexes containing chelated en (**4**, **5**) or acac (**6**−**8**) and Cl$^-$ as leaving group were synthesized in good yields via the Cl-bridged dimers, [($\eta^6$-arene)OsCl$_2$]$_2$ (**1**−**3**).

**X-ray Crystallography.** We determined the X-ray crystal structures of [($\eta^6$-bip)Os(en)Cl][BPh$_4$] (**4**), [($\eta^6$-bip)Ru(en)Cl][BPh$_4$] (**4R**),[26] [($\eta^6$-bip)Os(acac)Cl]·0.25CH$_3$OH (**6**·0.25CH$_3$OH), [($\eta^6$-bz)Os(acac)Cl] (**7**), and [($\eta^6$-*p*-cym)Os(acac)Cl] (**8**).[27] All have the familiar pseudo-octahedral "three-legged piano-stool" geometry, with Os$^{II}$ $\pi$-bonded to the arene ligand (the "seat") and $\sigma$-bonded to a chloride and a chelating ligand (the three "legs" of the piano stool). Crystallographic data are shown in Table S1, and selected bond lengths and angles are listed in Table S2. No intermolecular arene ring stacking is observed for any of these complexes.

The structures of the Os$^{II}$ complex **4** and Ru$^{II}$ complex **4R** containing chelated en are shown in Figure 1. They crystallize in the same monoclinic unit cell, space group *Cc*, with almost identical unit cell dimensions. The BPh$_4^-$ counterion in both **4** and **4R** sandwiches the chelated ethylenediamine, forming chains with short-range en(NH)···C(BPh$_4$) interactions of 3.424(5) Å (N(1)···C(16)) for **4** and 3.293(6) Å (N(8)···C(30)) for **4R** (see Figure S1). The metal−Cl (2.4015(9) and 2.4005(10) Å for **4** and **4R**, respectively), metal−N (2.108(3)−2.148(3) Å), and metal−C (2.149(4)−2.230(4) Å) bond lengths are similar for the two complexes (Table S2), as is the propeller twist of the biphenyl ligand (ca. 15°).

The structures of the Os$^{II}$ complexes **6**−**8** containing chelated acac are shown in Figure 2. The Os−Cl and Os−O bond lengths range from 2.4177(10) to 2.4222(10) Å and from 2.062(11) to 2.086(11) Å, respectively (Table S2). Complex **6** crystallizes with one-fourth solvent molecule of methanol and shows disorder in the coordinated biphenyl ring, which occupies three different positions (Figure S2), resulting in a lower quality of determination. For all of these conformations, the propeller twist of the biphenyl ligand is ca. 30°, and the pendent phenyl ring lies above the chelated acac ligand. Complex **7** shows disorder in the coordinated benzene ring over two different positions with equal occupancy (Figure S2). Two independent molecules of **8** crystallize in the same unit cell, but no disorder was observed for the coordinated *p*-cymene ring.

***Chart 1.*** Osmium Arene Complexes Studied in This Work

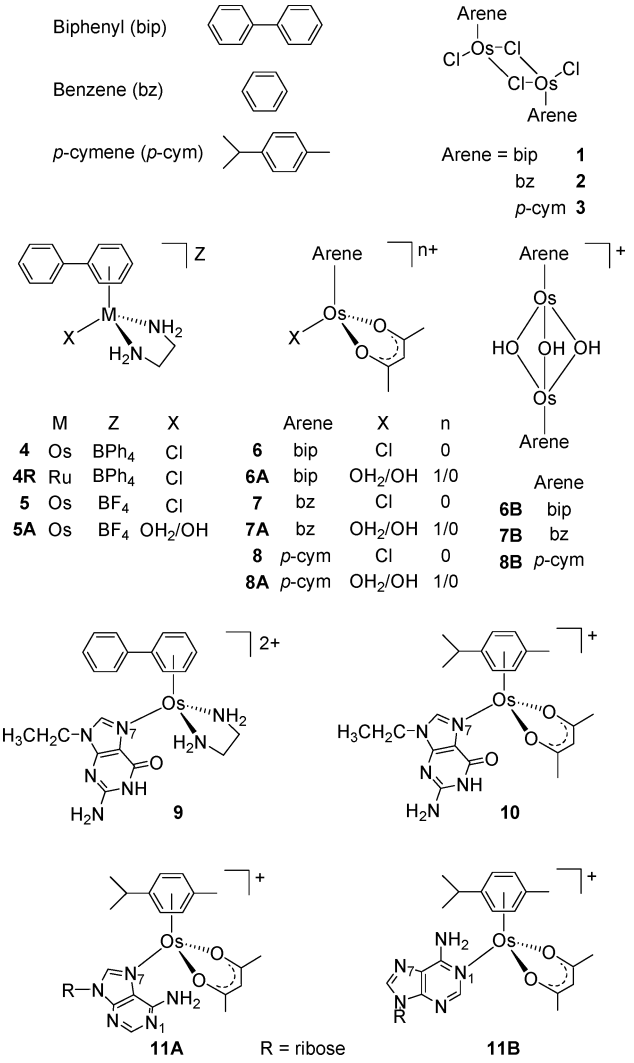


(23) *KALEIDAGRAPH*, version 3.09; Synergy Software: Reading, PA, 1997.
(24) Krezel, A.; Bal, W. *J. Inorg. Biochem.* **2004**, *98*, 161−166.
(25) Skehan, P.; Storeng, R.; Scudiero, D.; Monks, A.; McMahon, J.; Vistica, D.; Warren, J. T.; Bokesch, H.; Kenney, S.; Boyd, M. R. *J. Natl. Cancer Inst.* **1990**, *82*, 1107−1112.
(26) We reported previously the X-ray crystal structure of the PF$_6$ salt[8] but were able to crystallize the Os$^{II}$ complex only as a BPh$_4$ salt. Hence, we have now determined the X-ray structure of **4** so that direct comparison is possible.
(27) We reported previously the X-ray structure of the Ru analogue [($\eta^6$-*p*-cym)Ru(acac)Cl].[9]

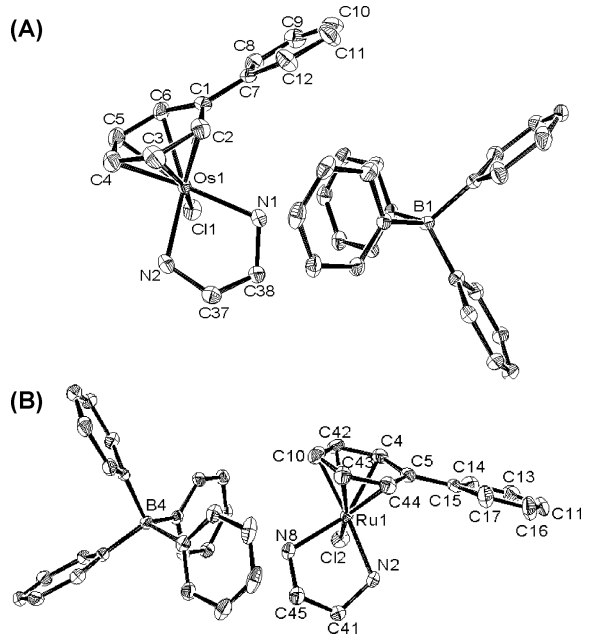


***Figure 1.*** ORTEP diagrams and atom numbering schemes for (A) [($\eta^6$-bip)Os(en)Cl][$BPh_4$] **(4)** and (B) [($\eta^6$-bip)Ru(en)Cl][$BPh_4$] **(4R)** (50% probability ellipsoids). The H atoms have been omitted for clarity. The sandwich formed by the phenyl rings of the counteranion and the en backbone is apparent.

An interesting feature of the crystal structures of complexes **6**−**8** is the directional hydrogen bonding ($\angle$D−H···A 150° < $\theta$ < 180°) between coordinated (arene)H and (acac)O atoms of adjacent molecules (Table 1), the shortest CH···O hydrogen bond being 2.29 Å for **6**. These hydrogen bonds are responsible for the formation of dimers (Figure S3).

**Hydrolysis.** The $^1$H NMR spectrum of the en complex **5**, [($\eta^6$-bip)Os(en)Cl][$BF_4$], in 5% MeOD-$d_4$/95% $D_2O$ at 298 K initially contained one major set of peaks. A second set of peaks increased in intensity with time, reaching equilibrium after ca. 30 h (Figure S4). The new peaks had chemical shifts similar to those of the aqua complex **5A**, prepared by treatment of **5** with $AgNO_3$, under the same conditions (arene peaks doublet $\delta$ 6.28, triplet $\delta$ 6.05, and triplet $\delta$ 5.96; pH* 7, Figure S5). Fitting the hydrolysis data to pseudo-first-order kinetics gave a half-life of 6.4 ± 0.2 h (298 K) (Figure 3).

In contrast, no peaks for the parent chloro complexes were observed in the $^1$H NMR spectra of ca. 2 mM solutions of the acac complexes **6**−**8** in $D_2O$ at 298 K. Within 10 min of dissolution, two major sets of peaks were seen in the arene region: **6A** (doublet $\delta$ 6.67, triplet $\delta$ 6.58, overlapped triplet $\delta$ 6.45) and **6B** (overlapped doublet $\delta$ 6.46, triplet $\delta$ 6.25, triplet $\delta$ 6.01), **7A** (singlet $\delta$ 6.28) and **7B** (singlet $\delta$ 6.03), and **8A** (doublets at $\delta$ 6.28 and $\delta$ 6.07) and **8B** (doublets at $\delta$ 6.04 and $\delta$ 5.82) (Figure 4). Peaks assignable to free acacH ($\delta$ 2.26) were also present in the spectra. The ESI-MS spectra of these NMR samples contained peaks at *m*/*z* 445 (**6A**) and 741 (**6B**), 370 (**7A**) and 591 (**7B**), and 426 (**8A**) and 701 (**8B**), assignable to the fragment [($\eta^6$-arene)Os(acac)]$^+$ arising from **6A**, **7A**, and **8A** (calcd *m*/*z* 445.1, 370.1, and 426.1, respectively) and to [($\eta^6$-arene)Os($\mu^2$-OH)$_3$Os($\eta^6$-arene)]$^+$ for **6B**, **7B**, and **8B** (calcd *m*/*z* 742.1, 590.0, and 701.1, respectively). Further confirmation of the assignment of the $^1$H NMR peaks for **6A**, **7A**, and **8A** to the aqua complexes [($\eta^6$-arene)Os(acac)($OH_2$)]$^+$ was obtained by recording the spectra of solutions of **6**, **7**, and **8** in $D_2O$ after addition of 1 mol equiv of $AgNO_3$ (and removal of AgCl by filtration).

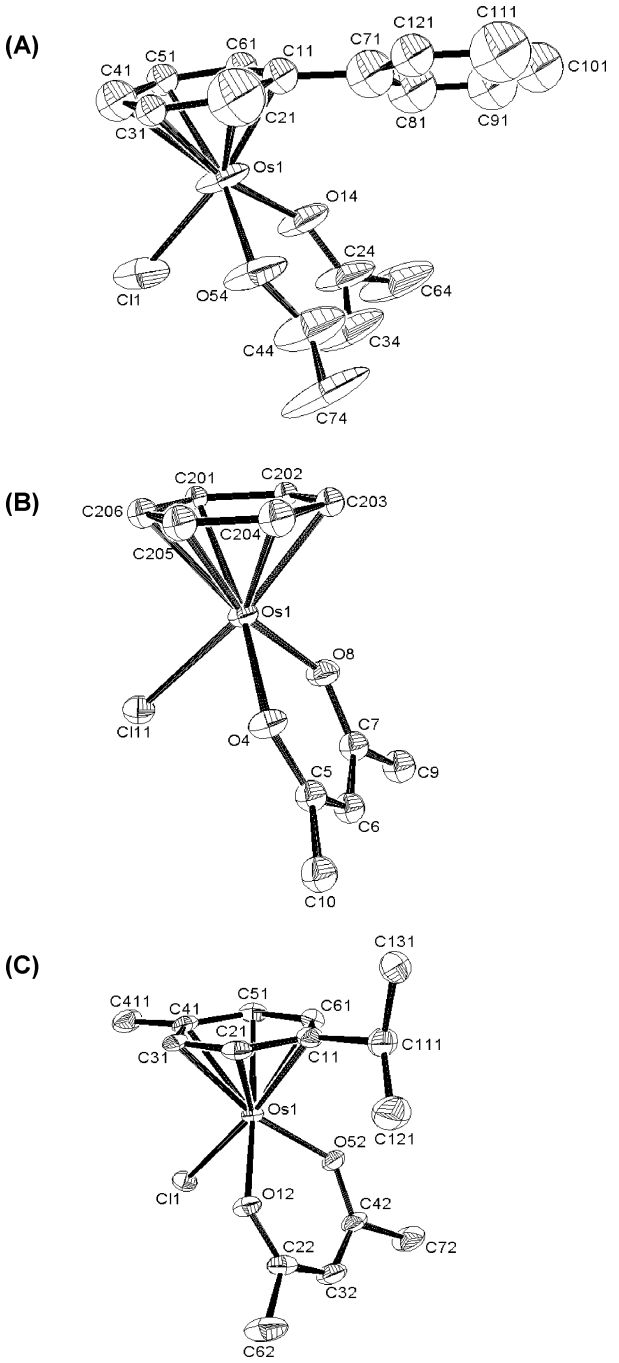


***Figure 2.*** ORTEP diagrams and atom numbering schemes for (A) [($\eta^6$-bip)Os(acac)Cl] **(6)**, (B) [($\eta^6$-bz)Os(acac)Cl] (**7**), and (C) [($\eta^6$-*p*-cym)Os-(acac)Cl] **(8)** (50% probability ellipsoids). The H atoms have been omitted for clarity. Two independent molecules of **8** crystallize in the same unit cell; only one is shown.

The effect of NaCl on the hydrolysis equilibrium for **8** was investigated. Addition of excess NaCl (to give 0.15 M) to an equilibrium solution of **8** (1.2 mM) in $D_2O$ caused the *p*-cymene $^1$H NMR peaks for species **8A** to shift from 6.26 and 6.05 ppm to 6.19 and 5.95 ppm, respectively, and broaden, whereas the peaks for species **8B** at 6.05 and 5.82 ppm remained unchanged. The resulting spectrum was similar to that obtained on dissolution of **8** in a 1 M NaCl solution in $D_2O$ (see Figure S6).

***Table 1.*** Selected Hydrogen-Bonding Interactions for Complexes **6**−**8**

| D−H···A | H···A (Å) | D···A (Å) | ∠D−H···A (°) |
|---|---|---|---|
| (A) [($\eta^6$-bip)Os(acac)Cl]·0.25$CH_3OH$ (**6**·0.25$CH_3OH$) | | | |
| C42−H42···O14 (inter) | 2.50 | 3.42(2) | 163 |
| C51−H51···O54 (inter) | 2.29 | 3.23(2) | 168 |
| (B) [($\eta^6$-bz)Os(acac)Cl] (**7**) | | | |
| C106−H1051···O4 (inter) | 2.34 | 3.332(13) | 169 |
| C201−H2043···O8 (inter) | 2.31 | 3.319(9) | 175 |
| (C) [($\eta^6$-*p*-cym)Os(acac)Cl] (**8**) | | | |
| C53−H53···O52 (inter) | 2.56 | 3.412(6) | 149 |
| C411−H41A···O14 (inter) | 2.60 | 3.565(7) | 169 |

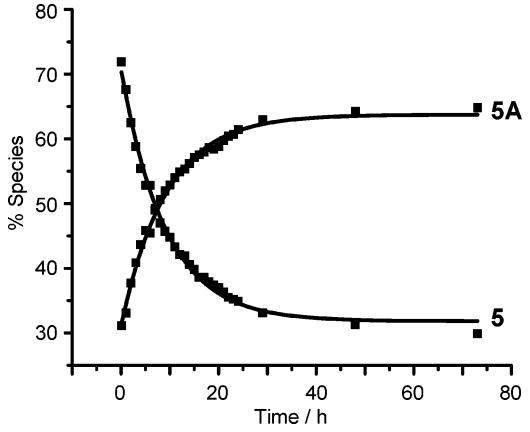


***Figure 3.*** Hydrolysis of [($\eta^6$-bip)Os(en)Cl]$BF_4$ (**5**). Time dependence of the decay of the chloro complex **5** and formation of the aqua/hydroxo adduct **5A** in 5% MeOD-$d_4$ 95% $D_2O$ at 298 K. The curves represent the computer best-fit for a pseudo-first-order reaction corresponding to an hydrolysis rate constant of 0.11 $h^{-1}$ (half-life of 6.4 ± 0.2 h).

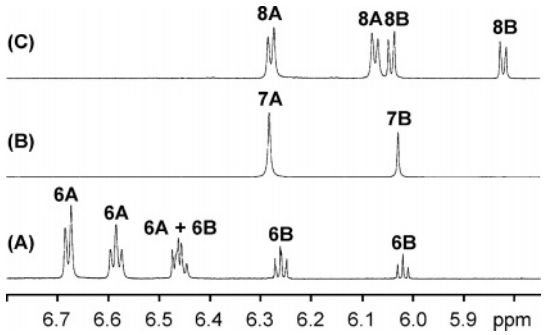


***Figure 4.*** Hydrolysis of the acac complexes [($\eta^6$-arene)Os(acac)Cl]. $^1$H NMR spectra of complexes (A) **6** (arene = bip), (B) **7** (arene = bz), and (C) **8** (arene = *p*-cym) in $D_2O$ recorded 30 min after dissolution at concentrations of 3.5, 2.1, and 3.4 mM, respectively, and 298 K. Two sets of peaks appear, corresponding to the aqua species, [($\eta^6$-arene)Os(acac)-$(OD_2)]^+$ (**6A**, **7A**, and **8A**), and the hydroxo-bridged dimers, [($\eta^6$-arene)-Os($\mu^2$-OD)$_3$Os($\eta^6$-arene)]$^+$ (**6B**, **7B**, and **8B**).

The $^1$H NMR spectra of solutions of **8**, [($\eta^6$-*p*-cym)Os(acac)-Cl], at low (micromolar) concentrations within the range used in the cytotoxicity tests were recorded. Spectra of **8** at 2 and 50 $\mu$M (in 0.125% DMSO-$d_6$/99.875% $D_2O$ (v/v), pH* 7.7) after ca. 30 min at 298 K and 24 h after incubation at 310 K contained only one set of peaks in the arene region ($\delta$ 6.04 and $\delta$ 5.82, Figure 5), assignable to species **8B**. Spectra recorded in the absence of DMSO-$d_6$ were the same. The ESI-MS of an equilibrium solution (Figure 5) contained a peak at *m*/*z* 704, confirming that the major species present is the hydroxo-bridged dimer, **8B**, [($\eta^6$-*p*-cym)Os($\mu^2$-OD)$_3$Os($\eta^6$-*p*-cym)]$^+$ (calcd *m*/*z* 703.9). We also recorded a $^1$H NMR spectrum of a 50 $\mu$M solution of

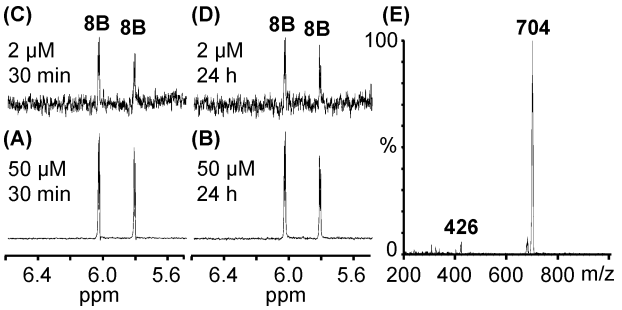


***Figure 5.*** Hydrolysis of [($\eta^6$-*p*-cym)Os(acac)Cl] (**8**) at micromolar concentrations. Low-field region of the $^1$H NMR spectra of a 50 $\mu$M solution of **8** in $D_2O$ (A) after 30 min at 298 K and (B) at 310 K after 24 h incubation at 310 K, and of a 2 $\mu$M solution of **8** (C) after 30 min at 298 K and (D) at 310 K after 24 h incubation at 310 K (biological test concentrations and conditions). Signals at $\delta$ 6.04 and 5.82 are assigned as *p*-cymene arene resonances of **8B**, [($\eta^6$-*p*-cym)Os($\mu^2$-OD)$_3$Os($\eta^6$-*p*-cym)]$^+$. (E) ESI-MS of sample from (B). The major peak at *m*/*z* 704 is assignable to the fragment [($\eta^6$-*p*-cym)Os($\mu^2$-OD)$_3$Os($\eta^6$-*p*-cym)]$^+$.

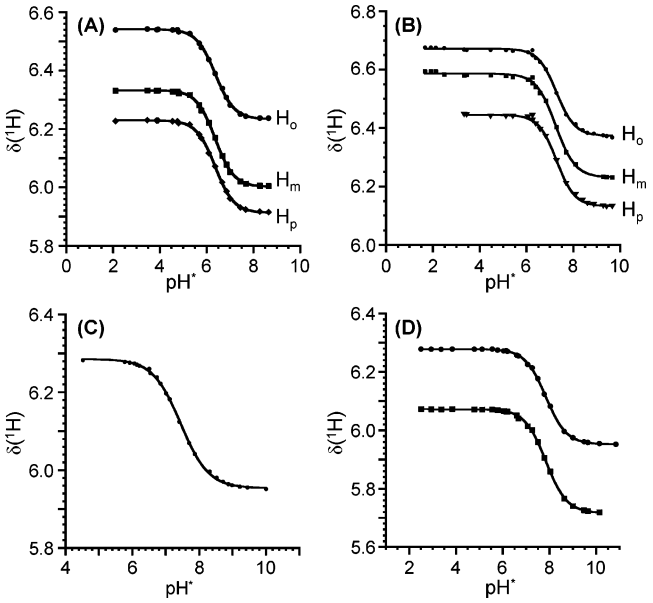


***Figure 6.*** Determination of the p$K_a$* values of the aqua complexes [($\eta^6$-arene)Os(LL)$(OD_2)]^{n+}$. Dependence of the $^1$H NMR chemical shifts of the coordinated arene ring on pH* for (A) [($\eta^6$-bip)Os(en)$(OD_2)]^{2+}$ (**5A**; ● ortho $H_o$, ■ meta $H_m$, ◆ para $H_p$), (B) [($\eta^6$-bip)Os(acac)$(OD_2)]^+$ (**6A**; ● ortho $H_o$, ■ meta $H_m$, ▼ para $H_p$), (C) [($\eta^6$-bz)Os(acac)$(OD_2)]^+$ (**7A**), and (D) [($\eta^6$-*p*-cym)Os(acac)$(OD_2)]^+$ (**8A**). The curves represent the best fits to the Henderson−Hasselbalch equation and correspond to p$K_a$* values of 6.37 for **5A**, 7.28 for **6A**, 7.45 for **7A**, and 7.84 for **8A**.

**8** in 0.15 M NaCl in $D_2O$ (mimicking the chloride concentration in cell culture media) at 298 K. Again, the only peaks present in the spectrum were those for the hydroxo-bridged dimer **8B**.

**pH* Dependence.** The changes in the $^1$H NMR chemical shifts of the coordinated phenyl ring of **5A** present in an equilibrium solution of **5** in $D_2O$ at 298 K (see Figure S4) were followed with change in pH* over the range 2−9. These data were fitted to the Henderson−Hasselbalch equation (Figure 6A), which yielded a p$K_a$* value of 6.37.

The pH* dependence of the $^1$H NMR chemical shifts of the coordinated arenes of complexes **6A/B**, **7A/B**, and **8A/B** was monitored over the range 2−10 (Figure 6). Those for species **6B**, **7B** and **8B** remained unchanged[28] with pH* (over the range 2−10), but their intensities increased with increase in pH* (Figure S7). In contrast, the peaks for **6A**, **7A**, and **8A** shifted

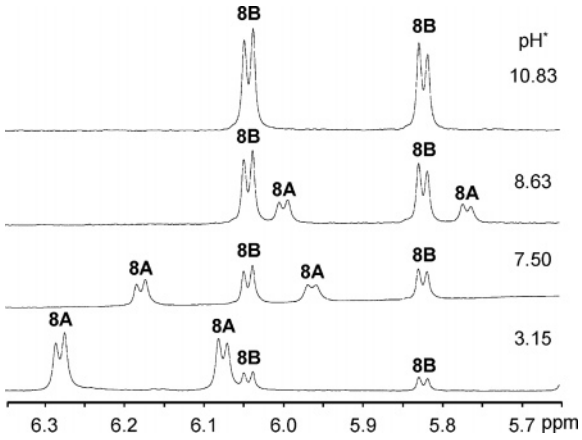


***Figure 7.*** Formation of hydroxo-bridged dimer from the aqua complex $[(\eta^6\text{-}p\text{-cym})Os(acac)(OD_2)]^+$. $^1H$ NMR spectra recorded during a pH titration of a solution of the chloro complex **8** in $D_2O$, containing predominantly the aqua/hydroxo complex **8A** ($[(\eta^6\text{-}p\text{-cym})Os(acac)(OD_2/OD)]^{+/0}$) and the dimer **8B** ($[(\eta^6\text{-}p\text{-cym})Os(\mu^2\text{-OD})_3Os(\eta^6\text{-}p\text{-cym})]^+$), showing how the peaks for **8B** increase in intensity with increasing pH* but do not shift, whereas those for **8A** shift to high field (deprotonation, fast exchange between aqua and hydroxo forms) and decrease in intensity as conversion into the dimer occurs.

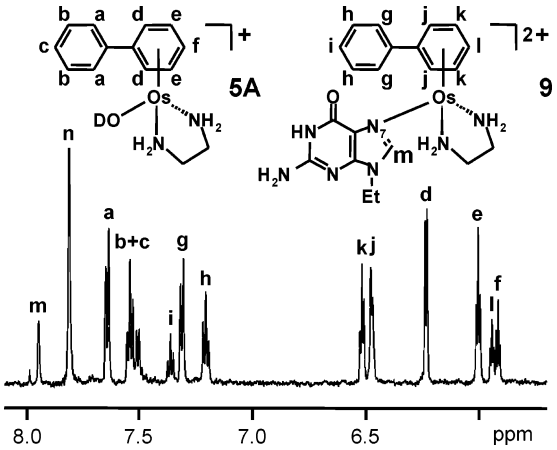


***Figure 8.*** Reaction of 9-ethylguanine with $[(\eta^6\text{-bip})Os(en)(OD_2/OD)]^{2+/+}$ (**5A**) (at pH* 7.28, mostly in the hydroxo form). Low-field region of the $^1H$ NMR spectrum of **5A** (formed by treating a solution of the chloro complex **5** with 1 mol equiv of $AgNO_3$) after reaction with 2 mol equiv of 9-EtG in $D_2O$ at 298 K for 22 h. At this time, 45% of **5A** had reacted to form **9** ($[(\eta^6\text{-bip})Os(en)(9\text{-EtG-}N7)]^{2+}$). Peak labels correspond to the structures; peak n is from H8 of unbound 9-EtG.

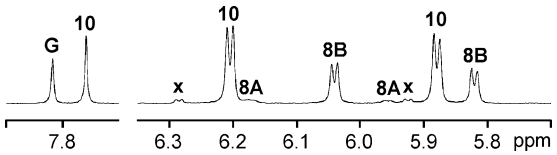


***Figure 9.*** Reaction of 9-ethylguanine with $[(\eta^6\text{-}p\text{-cym})Os(acac)Cl]$ (**8**). Low-field region of the $^1H$ NMR spectrum of **8** after reaction with 1 mol equiv of 9-EtG in $D_2O$, 298 K, at equilibrium (within ca. 10 min of reaction). Peak labels: **G**, unreacted 9-EtG (corresponds to 40% of total 9-EtG); **10**, $[(\eta^6\text{-}p\text{-cym})Os(acac)(9\text{-EtG-}N7)]^+$ (60%); **8A**, unreacted aqua complex $[(\eta^6\text{-}p\text{-cym})Os(acac)(OD_2)]^+$ (7%); **8B**, dimer $[(\eta^6\text{-}p\text{-cym})Os(\mu^2\text{-OD})_3Os(\eta^6\text{-}p\text{-cym})]^+$ (33%); **x**, an unidentified product.

to high field and decreased in intensity with increase in pH* (Figure 7), the maximum shift change being ca. 0.3 ppm in each case. These data yielded $pK_a$* values of 7.28, 7.45, and 7.84 for the biphenyl complex **6A**, benzene complex **7A**, and *p*-cymene complex **8A**, respectively (Figure 6B−D).

Analysis of peak integrals of $^1H$ NMR spectra showed that millimolar solutions of **8** in $D_2O$ at pH* 2.1 contained mostly **8A**, and only 4% of **8B**. On raising the pH* to 10.2, very little of **8A** remained and the proportion of **8B** increased to 78%. However, on lowering the pH* to 2.5, the amount of **8A** present remained the same but the proportion of **8B** fell to 33%, and peaks for unidentified species $x_1$ and $x_2$ (which were minor components in the initial solution at pH* 2.1) increased in intensity (see Figure S8). At pH* 11.8, only peaks for **8B** and free acac were observed (Figure S8).

**Interactions with Nucleobases.** Since DNA is a potential target site for transition metal anticancer complexes,[29] reactions with model nucleobases were studied.

Addition of 1 mol equiv of 9-EtG to an equilibrium solution of complex **5**, $[(\eta^6\text{-bip})Os(en)Cl][BF_4]$, in $D_2O$ (pH* 7.28) at 298 K resulted in no new $^1H$ NMR peaks after 10 min. After 22 h, 23% of **5** had reacted and a new H8 peak appeared at 8.09 ppm (for species **9**, see Figure S9), shifted by 0.27 ppm to low field relative to that of free 9-EtG. Addition of 2 mol equiv of 9-EtG to a solution of **5A** (pH* 7.0) (prepared by treating a solution of **5** with 1 mol equiv of $AgNO_3$) also resulted in no new $^1H$ NMR peaks after 10 min, but after 22 h new peaks assignable to **9** had appeared, and 45% of **5A** had reacted with 9-EtG to form **9** (Figures 8 and S10).

The addition of a solution of 1 mol equiv of adenosine (Ado), cytidine (Cyt), or thymidine (Thy) to an equilibrium solution of **5** in $D_2O$ at 298 K resulted in no additional $^1H$ NMR peaks over a period of 24 h (Figure S11).

Addition of 1 mol equiv of 9-EtG in $D_2O$ to an equilibrium solution of the acac complex **8**, $[(\eta^6\text{-}p\text{-cym})Os(acac)Cl]$, in $D_2O$ (which contained 70% aqua complex **8A** and 30% hydroxo-bridged dimer **8B**, together with some free acacH) at 298 K, pH* 7.50, resulted in a new set of $^1H$ NMR peaks (for species **10**, see Figures 9 and S12) within 10 min (by which time equilibrium had been reached). Peaks for **8A** diminished in intensity, but those for **8B** did not change. Based on H8 peak integrals for free ($\delta$ 7.82) and bound ($\delta$ 7.76) 9-EtG, 60% of the 9-EtG reacted to form **10**. The major ESI-MS peak for the equilibrium NMR sample at a low cone voltage (10 V) was at *m*/*z* 605, consistent with the formation of $[(\eta^6\text{-}p\text{-cym})Os(acac)(9\text{-EtG-}N7)]^+$ (**10**, calcd *m*/*z* 605.2) (see Figure 10). To establish the binding site for $Os^{II}$ on 9-EtG, a pH* titration of the reaction mixture was monitored by $^1H$ NMR spectroscopy over the range pH* 2−8 (Figure 11). The chemical shift of H8 for **10** did not change with pH*, whereas that of free 9-EtG moved to high field by ca. 1 ppm, corresponding to a $pK_a$* of 3.26, consistent with values for N7 protonation reported previously.[30]

No new $^1H$ NMR peaks appeared in the spectrum of **8** on addition of 1 mol equiv of 9-EtG under more alkaline conditions, where the hydroxo-bridged dimer **8B** predominates (pH* 9.9, >95% **8B**), even after 96 h, indicative of the inertness of **8B**.

Addition of a solution of 1 mol equiv of Ado to an equilibrium solution of **8** in $D_2O$ (which contain 70% aqua

(28) The intensity of the $^1H$ NMR peak for the acacH methyl protons decreases at basic pH* as they exchange readily with D from the solvent, as reported previously: Johnson, D. A. *Inorg. Chem.* **1966**, *5*, 1289−1291. The central $\gamma$ proton exchanges readily with $D_2O$ even at neutral pH*.

(29) Zhang, C. X.; Lippard, S. J. *Curr. Opin. Chem. Biol.* **2003**, *7*, 481−489.

(30) Kampf, G.; Kapinos, L. E.; Griesser, R.; Lippert, B.; Sigel, H., *J. Chem. Soc., Perkin Trans. 2* **2002**, 1320−1327.

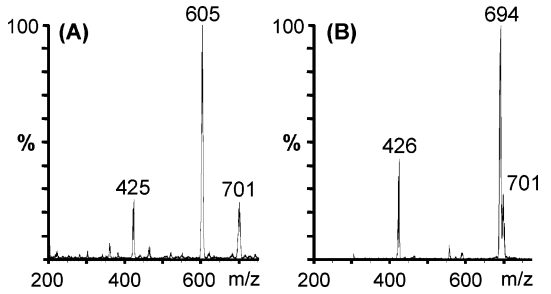


***Figure 10.*** Characterization of 9-ethylguanine and adenosine adducts by mass spectrometry. ESI mass spectra for solutions containing [($\eta^6$-*p*-cym)-Os(acac)Cl] (**8**) and 1 mol equiv of (A) 9-ethylguanine and (B) adenosine in $D_2O$. Peaks at *m*/*z* 425/426 correspond to **8A** ([($\eta^6$-*p*-cym)Os(acac)]$^+$), *m*/*z* 701 to the hydroxo-bridged dimer **8B**, and 605 and 694 to **10** ([($\eta^6$-*p*-cym)Os(acac)(9-EtG)]$^+$) and **11** ([($\eta^6$-*p*-cym)Os(acac)(Ado)]$^+$), respectively.

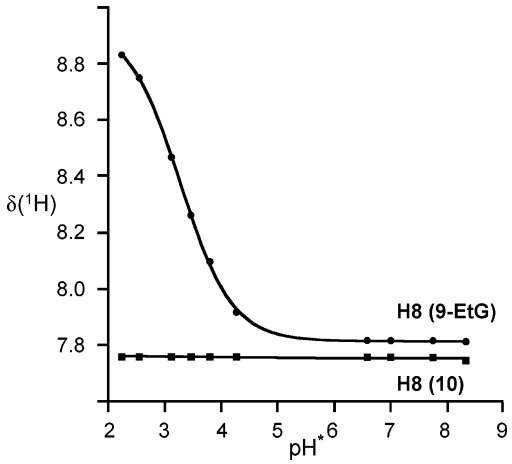


***Figure 11.*** Determination of {($\eta^6$-*p*-cym)Os(acac)}$^+$ binding site on 9-ethylguanine. Dependence of the $^1$H NMR chemical shift of 9-EtG H8 on pH* for a solution containing **10** ([($\eta^6$-*p*-cym)Os(acac)(9-EtG-*N7*)]$^+$) and free 9-EtG. The lack of pH* dependence for **10** over the pH* range from 5 to 2, where N7 protonates, confirms that binding of 9-EtG to Os$^{II}$ is through N7.

complex **8A**, 30% hydroxo-bridged dimer **8B**, and some free acacH) at 298 K (pH* 7.31) led to the appearance of new peaks within 10 min (Figure 12A), assignable to a major product **11A** (accounting for 56% of Ado) and a minor product **11B** (10% of Ado). In the H8/H2 region, two new sets of peaks appeared at 8.50 and 8.31 ppm for **11A** and at 8.39 and 8.17 ppm for **11B**. ESI-MS studies of this NMR sample at a low cone voltage (20 V) gave a peak at *m*/*z* 694, consistent with [($\eta^6$-*p*-cym)-Os(acac)(Ado)]$^+$ (**11**, calcd *m*/*z* 694.2) (Figure 10). The binding sites for {($\eta^6$-*p*-cym)Os(acac)}$^+$ on Ado in **11A** and **11B** were assigned with the aid of a $^1$H NMR pH* titration of the reaction mixture over the pH* range from 7 to 1 (Figure 12B). The singlets for H8 and H2 of free Ado shifted to low field with an associated p$K_a$* of 3.63, a value similar to that reported previously for N1 protonation,[30] whereas the H8 and H2 peaks for **11B** did not shift over this pH* range, consistent with the presence of N1-bound Ado in this complex, [($\eta^6$-*p*-cym)Os-(acac)(Ado-*N1*)]$^{2+}$. Those for **11A** shifted to low field over this pH* range with an associated p$K_a$* value of 1.92, assignable to N1 protonation of N7-bound Ado. This corresponds to a lowering of the p$K_a$* of N1 by 1.7 units for **11A** [($\eta^6$-*p*-cym)-Os(acac)(Ado-*N7*)]$^{2+}$ compared to free Ado. Interestingly, the arene peaks for **11A** are greatly broadened (Figure 12A; no significant sharpening over the temperature range 298−323 K).

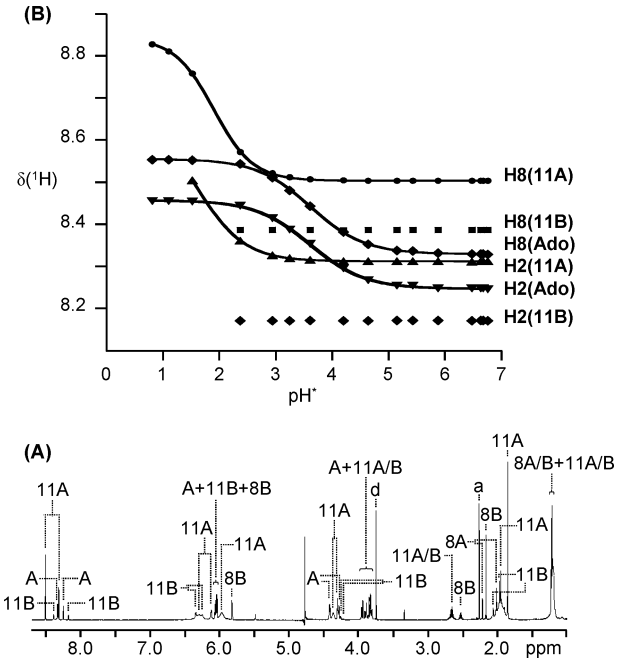


***Figure 12.*** Reaction of [($\eta^6$-*p*-cym)Os(acac)Cl] (**8**) with adenosine. (A) $^1$H NMR spectrum of a $D_2O$ solution of **8** and 1 mol equiv of adenosine, pH* 7.31, 298 K, at equilibrium (within ca. 10 min of reaction). (B) Dependence of the $^1$H NMR chemical shifts of Ado H8 and H2 resonances on pH*. Assignments: **8B**, hydroxo-bridged dimer [($\eta^6$-*p*-cym)Os($\mu^2$-OD)$_3$-Os($\eta^6$-*p*-cym)]$^+$; **8A** aqua complex [($\eta^6$-*p*-cym)Os(acac)(OD$_2$)]$^+$; **A**, unreacted adenosine (Ado); **d**, dioxane, **a**, free acacH; **11A**, major product, [($\eta^6$-*p*-cym)Os(acac)(Ado-*N7*)]$^{2+}$; **11B**, minor product, [($\eta^6$-*p*-cym)Os(acac)(Ado-*N1*)]$^{2+}$. Based on peak integration, 66% Ado has reacted to give 56% **11A** and 10% **11B**. Binding through N7 lowers the p$K_a$* of N1 by ca. 1.7 pH units.

The addition of 1 mol equiv of Cyt or Thy to an equilibrium solution of **8** in $D_2O$ at 298 K resulted in no additional $^1$H NMR peaks over a period of 24 h (Figure S13).

**Cytotoxicity toward A2780 and A549 Human Cancer Cells.** Complexes **4**, **5**, and **8** were all nontoxic toward the human ovarian A2780 cancer cell line at concentrations up to 50 $\mu$M (the highest test concentration). The $IC_{50}$ values are therefore likely to be >100 $\mu$M, and the complexes are inactive. Similarly complexes **6**−**8** were found to be inactive against the human lung A549 cancer cell line.

## Discussion

**X-ray Crystallography.** A search of the Cambridge Database revealed that only ca. 200 structures of osmium arene complexes have been reported, compared to ca. 3000 for ruthenium arene complexes. The crystal structures of complexes **4** and **6** are the first to be reported with $\eta^6$-biphenyl coordination to osmium, and **4** is the first containing an {($\eta^6$-arene)Os(en)} fragment.

The Os$^{II}$ (**4**) and Ru$^{II}$ (**4R**) en complexes are isostructural in the solid state. The M−Cl bond lengths are the same (2.40 Å), even though the ligand exchange rates are different. Similarly, the Os$^{II}$ acac complex **8** and its Ru$^{II}$ analogue [($\eta^6$-*p*-cym)Ru-(acac)Cl], which we reported previously,[9] have similar M−Cl and M−O bond lengths.

Hydrogen bonds are observed between (arene)H and (acac)O of adjacent molecules in the crystal structures of osmium complexes **6**−**8**, giving rise to dimers (Figure S3). Such H-bonds involving coordinated arenes are becoming increasingly recognized.[31] We observed them previously[9] for [($\eta^6$-*p*-cym)Ru(acac)-

Cl], and they are also present (but not often noted) in the crystal structures of other reported $Os^{II}$ arene acac complexes.[32] Hydrogen bonds can be distinguished from van der Waals interactions by their directional nature ($\angle D-H\cdots A$ $150° < \theta < 180°$), as they consist of both van der Waals and electrostatic components.[33] C−H···O H-bonds are typically given cutoff values of <2.6 Å.[34] They are weaker than classical hydrogen bonds, and present only in the absence of stronger interactions, but can direct crystal packing.[35] The weak polarization of arene ring C−H bonds may lead to interactions between the coordinated arene and H-bond acceptors in biological target sites such as DNA or RNA.

**Hydrolysis.** There are few previous studies of the aqueous chemistry of $Os^{II}$ arene complexes.[13−15] The hydrolysis of the $Os^{II}$ en complex **5** in water (Figure 3, half-life of 6.4 h) is ca. 40 times slower than that of its $Ru^{II}$ analogue.[12] This behavior is consistent with the much slower ligand exchange rates often associated with osmium complexes in comparison with those of ruthenium. However, Stebler-Röthlisberger et al. found that the $Os^{II}$ and $Ru^{II}$ complexes $[(\eta^6\text{-bz})M(OH_2)_3]^{2+}$, without a chelating ligand, possess similar water exchange rates.[14] The presence of a chelating ligand can introduce significant differences between $Os^{II}$ and $Ru^{II}$.

Changing the chelating ligand from en to acac in $Os^{II}$ arene complexes had a marked effect on the extent and rate of hydrolysis, as is also the case for $Ru^{II}$ analogues.[9] However, hydroxo-bridged dimers play a dominant role in the hydrolysis behavior of $[(\eta^6\text{-arene})Os(acac)Cl]$ complexes in water (complexes **6B**, **7B**, and **8B** are products from the hydrolysis of the bip, bz, and *p*-cym complexes **6**, **7**, and **8**, respectively), whereas they are only minor components, and then only at high pH*, in analogous $Ru^{II}$ systems.[9] There appear to be no previous reports of the formation of hydroxo-bridged $Os^{II}$ arene complexes on dissolution of $Os^{II}$ arenes in water, although the dimers[36] have been synthesized by heating $[\eta^6\text{-arene})OsCl_2]_2$ in strongly alkaline solutions.[36c,e] X-ray structures of $[(\eta^6\text{-arene})Ru(\mu^2\text{-OH})_3\text{-}Ru(\eta^6\text{-arene})]^+$ have been reported,[36d,f−h] although the only X-ray structure of a hydroxo-bridged $Os^{II}$ arene dimer appears to be that of $[(\eta^6\text{-}p\text{-cym})Os(\mu^2\text{-H})(\mu^2\text{-HCO}_2)(\mu^2\text{-OH})Os(\eta^6\text{-}p\text{-cym})]^+$.[36e] For (sterically nonhindered) benzene as the arene ligand, further deprotonation of hydroxo bridges appears to be possible to give the tetramer $[M_4(\eta^6\text{-bz})(\mu^2\text{-OH})_4(\mu^4\text{-O})]^{2+}$ (M = Ru or Os).[36a,b,d] We found no (ESI-MS) evidence for such tetramers under the less alkaline conditions used in this work. In contrast to $Ru^{II}$, the hydroxo-bridged dimer was still detectable in highly acidic millimolar solutions of $Os^{II}$ acac complexes (pH* 2).

***Table 2.*** p$K_a$ Values for $[(\eta^6\text{-Arene})M(chelate)(OH_2)]^{n+}$, $[(\eta^6\text{-bip})Os(en)(OH_2)]^{2+}$ (**5A**), $[(\eta^6\text{-bip})Os(acac)(OH_2)]^+$ (**6A**), $[(\eta^6\text{-bz})Os(acac)(OH_2)]^+$ (**7A**), $[(\eta^6\text{-}p\text{-cym})Os(acac)(OH_2)]^+$ (**8A**), and Some Ruthenium Arene Aqua Complexes

| complex | metal | arene | chelate | p$K_a$ |
|---|---|---|---|---|
| **5A** | Os | bip | en | 6.34[a] |
| | Ru | bip | en | 7.71[b] |
| | Ru | bz | en | 7.9[c] |
| | Os | bz | en | 6.3[d] |
| **6A** | Os | bip | acac | 7.12[a] |
| **7A** | Os | bz | acac | 7.27[a] |
| **8A** | Os | *p*-cym | acac | 7.63[a] |
| | Ru | *p*-cym | acac | 9.4[d] |

[a] p$K_a$ values calculated from p$K_a$* according to ref 18. [b] Reference 12. [c] Reference 13. [d] Reference 9.

Particularly relevant to the biological testing is our finding that the hydroxo-bridged dimer (**8B**) is the only species present on dissolution of $[(\eta^6\text{-}p\text{-cym})Os(acac)Cl]$ (**8**) in water at micromolar concentrations. The chelated acac ligand is readily protonated (e.g., by an adjacent coordinated aqua ligand in **8A**) and a good leaving group at acidic or near neutral pH (p$K_a$ of free acacH is 8.8[37]). In strongly basic solution, hydroxide appears to displace acac. The high stability of the hydroxo-bridged dimer is further illustrated by the finding that it is still formed as a major species, even in the presence of a large molar excess of $Cl^-$ (3000-fold, concentrations similar to those in cell culture media). In contrast, ring-opening of chelated en requires cleavage of the Os−N bond before protonation can occur, and en is not readily displaced by hydroxide.

We observed separate $^1$H NMR peaks for the $OH_2$/OH and the parent Cl complexes in the spectrum of the $Os^{II}$ en complex **5** on dissolution in $D_2O$. At millimolar concentrations of the $Os^{II}$ acac complex **8**, the $^1$H NMR chemical shifts are consistent with the existence largely of the aqua complex **8A** (confirmed by addition of $AgNO_3$), with little of the chloro complex present. Only one set of $^1$H NMR peaks was observed for solutions containing the acac aqua complex **8A** and Cl species **8**, suggesting rapid exchange of $Cl^-$ and coordinated $OH_2$/OH on the NMR time scale at 298 K, as observed for ruthenium analogues.[9] Addition of a large excess of chloride shifted and broadened these signals (Figure S6), suggesting that chloride binding to $\{(\eta^6\text{-}p\text{-cym})Os(acac)\}^+$ is indeed weak.

**p$K_a$* Values of Aqua Complexes.** The p$K_a$* values of the en $(\eta^6\text{-arene})Os^{II}$ aqua complex **5A** (6.37) and acac aqua complexes **6A**, **7A**, and **8A** (7.28, 7.45, and 7.84, Table 2) are all significantly lower (ca. 1.5 units) than those of analogous $(\eta^6\text{-arene})Ru^{II}$ aqua complexes.[9,38] The trend in the lowering of p$K_a$ values for $Os^{II}$ versus $Ru^{II}$ complexes is consistent with that reported previously for $([(\eta^6\text{-bz})M^{II}(OH_2)_3]^{2+}$ and $[M^{II}(trpy)(bipy)(OH_2)]^{2+}$ (trpy = 2,2′,2″-terpyridine, bipy = 2,2′-bipyridine).[13,38] The replacement of the neutral chelated en ligand by an anionic acac raises the p$K_a$* by 0.9 unit. A similar decrease in acidity is observed for the Ru analogues ($\Delta$p$K_a$ 1.1 units),[9] attributable to the increased electron density on the metal center. The higher acidity of $Os^{II}$ arene aqua complexes can be attributed to increased mixing of the $\delta\sigma^*$ (Os) → $\sigma$ ($OH^-$) orbitals.[38] The p$K_a$* values of the acac complexes **6A**, **7A**, and **8A** are close to physiological pH (7.4), whereas that of the en

(31) Braga, D.; Grepioni, F.; Desiraju, G. R. *J. Organomet. Chem.* **1997**, *548*, 33−44.
(32) Bennett, M. A.; Mitchell T. R. B.; Stevens M. R.; Willis A. C. *Can. J. Chem.* **2001**, *79*, 655−669.
(33) Steiner, T.; Desiraju, G. R. *Chem. Commun.* **1998**, 891−892.
(34) Steiner, T. *Chem. Commun.* **1997**, 727−734.
(35) Desiraju, G. R. *Acc. Chem. Res.* **1996**, *29*, 441−449.
(36) (a) Gould, R. O.; Jones, C. L.; Robertson, D. R.; Stephenson, T. A. *J. Chem. Soc., Chem. Commun.* **1977**, 222−223. (b) Gould, R. O.; Jones, C. L.; Robertson, D. R.; Tocher, D. A.; Stephenson, T. A. *J. Organomet. Chem.* **1982**, *226*, 199−207. (c) Arthur, T.; Robertson, D. R.; Tocher, D. A.; Stephenson, T. A. *J. Organomet. Chem.* **1981**, *208*, 389−400. (d) Gould, R. O.; Jones, C. L.; Stephenson, T. A.; Tocher, D. A. *J. Organomet. Chem.* **1984**, *264*, 365−378. (e) Cabeza, J. A.; Smith, A. J.; Adams, H.; Maitlis, P. M. *J. Chem. Soc., Dalton Trans.* **1986**, 1155−1160. (f) Vieille-Petit, L.; Therrien, B.; Süss-Fink, G. *Inorg. Chem. Commun.* **2004**, 232−234. (g) Kim, T. D.; McNeese, T. J.; Rheingold, A. L. *Inorg. Chem.* **1988**, *27*, 2554−2555. (h) Artero, V.; Proust, A.; Herson, P.; Gouzerh, P. *Chem. Eur. J.* **2001**, *7*, 3901−3910.
(37) Kortly, S.; Sucha, L. *Handbook of Chemical Equilibria in Analytical Chemistry*; Ellis Horwood Limited: New York, 1985; p 188.
(38) Takeuchi, K. J.; Thompson, M. S.; Pipes, D. W.; Meyer, T. J. *Inorg. Chem.* **1984**, *23*, 1845−1851.

complex **5A** is significantly lower, and therefore almost all of the hydrolyzed en complex would be present in the hydroxo form, $[(\eta^6\text{-bip})Os^{II}(en)(OH)]^+$.

**Interactions with Nucleobases.** There is little reported work on interactions of osmium complexes and nucleobases. Osmium(II) polypyridyl complexes are known to bind to DNA and nucleobases,[39−41] and recently adducts of $[(\eta^6\text{-}p\text{-cym})OsCl_2(PR_3)]$, where $PR_3$ = pta or pta-Me (pta = 1,3,5-triaza-7-phosphatricyclo[3.3.1.1]decane), with the 14 mer ATACATGGTACATA have been detected by ESI-MS.[42]

The Os$^{II}$ en complex **5** reacts only slowly with 9-EtG, as does the aqua complex **5A**, and then only to a limited extent (45% after 22 h at 298 K). No reaction was observed (after 24 h) with Ado, Cyt, or Thy. The Ru$^{II}$ analogue also binds selectively to guanine when in competition with the other three bases, but it does bind weakly to Cyt and Thy, highlighting the lower reactivity of Os$^{II}$. The aqua acac Os$^{II}$ adduct **8A** reacts with both 9-EtG and Ado rapidly (<10 min), but not with Cyt or Thy, a behavior similar to that of the Ru$^{II}$ analogue.[9] Binding to 9-EtG occurs through N7 and to Ado[43] through N7 and N1 (with N7 binding being favored by a factor of ca. 6:1; cf. 4:1 for Ru$^{II}$). Binding to Ado N7 lowers the p$K_a$* of N1 by 1.7 pH* units, compared to 1.3 for Ru$^{II}$.[9] This trend is similar to the lowering of p$K_a$ values of water coordinated to Os$^{II}$ compared to Ru$^{II}$. The selectivity in nucleobase binding of the Os$^{II}$ en and acac complexes can be rationalized in terms of H-bonding and nonbonding repulsive interactions between the chelating ligand and nucleobase substituents in addition to the electronic properties of the various nucleobase coordination sites,[44] as we have discussed previously for the Ru$^{II}$ analogues.[9,45] The inertness of the hydroxo-bridged dimer **8B** toward nucleobases is notable.

**Cytotoxicity toward A2780 and A549 Human Cancer Cell Lines.** None of the Os$^{II}$ arene en or acac complexes studied here (Chart 1) were cytotoxic to human ovarian or lung cancer cells at doses up to 50 $\mu$M, in contrast to their Ru$^{II}$ analogues, cf. $IC_{50}$ value for **4R** (analogue of **4**) of 5 $\mu$M and for $[(\eta^6\text{-}p\text{-cym})Ru(acac)Cl]$ (analogue of **8**) of 19 $\mu$M.[11] The inactivity of the Os$^{II}$ en complex **5** may be attributable to its much slower hydrolysis (ca. 40 times) and to the higher acidity of the aqua complex (ca. 1.4 p$K_a$ units) compared to the Ru$^{II}$ analogue.[12] This results in lower reactivity, e.g., toward nucleobases. Changing the chelating ligand to acac not only increases the hydrolysis rate dramatically but also lowers the acidity of the aqua adduct, such that a significant amount of the aqua complex (as opposed to the hydroxo adduct) exists at biological pH (7.4). These aqua acac complexes bind to purine bases, as do the Ru$^{II}$ analogues.[9] However, displacement of the coordinated acac from Os$^{II}$ occurs readily, and largely irreversibly, giving rise to stable hydroxo-bridged dimers. These inert dimers appear to be the only species present in solution under biological testing conditions and may account for the inactivity of the Os$^{II}$ acac complexes toward human cancer cells.

## Conclusions

We have shown previously that organometallic Ru$^{II}$ arene complexes such as $[(\eta^6\text{-arene})Ru(LL)Cl]^+$, where arene is, for example, biphenyl, benzene, or *p*-cymene and LL is en or acac, exhibit anticancer activity.[8,11] However, we report here that the Os$^{II}$ analogues are inactive toward A2780 human ovarian and A549 human lung cancer cells, despite being structurally very similar in the crystalline state. We have therefore explored differences in their solution chemistry in an attempt to understand their contrasting biological activities. There are few previous investigations of the aqueous chemistry of osmium arenes.[13−15] In general, as a third-row transition metal ion, Os$^{II}$ might be expected to be relatively inert compared to the second-row ion Ru$^{II}$.[17] However, the presence of an arene ligand can greatly increase the kinetic lability,[14] and, importantly, our data show that the chelating ligand also plays a major role.

With en as the chelating ligand, hydrolysis of the Os$^{II}$ complex **5** is ca. 40 times slower than that of the Ru$^{II}$ analogue, and the p$K_a$ value (6.34) of the resulting aqua adduct is 1.4 units lower. This implies that the less-reactive hydroxo adduct would predominate at physiological pH (7.4). Indeed, reactions with 9-EtG were slower and occurred to a lesser extent than those of the Ru$^{II}$ complexes. Since G bases on DNA appear to be targets for $\{(\eta^6\text{-arene})Ru(en)\}^{2+}$, these differences may account for biological inactivity of the Os$^{II}$ en complexes.

In contrast, the acac complexes $[(\eta^6\text{-arene})Os(acac)Cl]$ hydrolyze rapidly (<10 min, 298 K) to give a mixture of a monoaqua complex, $[(\eta^6\text{-arene})Os(acac)(OH_2)]^+$, and a hydroxo-bridged dimer, $[(\eta^6\text{-arene})Os(\mu^2\text{-}OH)_3Os(\eta^6\text{-arene})]^+$, with loss of the acac ligand. The p$K_a$ values of the coordinated water molecules in the monoaqua acac biphenyl, benzene, and *p*-cymene complexes (**6A**, **7A**, and **8A**, 7.1−7.6) are ca. 1.8 units lower than those of the Ru$^{II}$ analogues, for which the hydroxo-bridged dimer is not observed as an hydrolysis product (except in very basic solutions, and then only as a very minor product).

The monoaqua acac complex, **8A**, reacts with purine bases (9-EtG and Ado), but not with pyrimidines (Cyt or Thy); this is the same base selectivity that was observed for the Ru$^{II}$ analogues.[9] However, the hydroxo-bridged dimer, $[(\eta^6\text{-arene})Os(\mu^2\text{-}OH)_3Os(\eta^6\text{-arene})]^+$, was unreactive toward both purine and pyrimidine bases. This may be the key to the inactivity of the Os$^{II}$ arene acac complexes, since the hydroxo-bridged dimer was the only species present in micromolar aqueous solutions similar to those used in the biological tests.

This work demonstrates how the kinetics of ligand substitution reactions of Os$^{II}$ arene complexes in aqueous solution can be controlled by variation of the chelating ligand. Further tuning of substitution rates may be achievable by variations of the monodentate leaving group and the arene. Such a systematic approach should contribute to the rational design of Os$^{II}$ arene complexes as potential anticancer agents and may be more widely applicable to organometallic complexes in general.

**Acknowledgment.** We thank the EPSRC and The University of Edinburgh (studentship for A.F.A.P.), the EC (Marie Curie Fellowship for R.F.), and The Wellcome Trust for support, Michael Melchart (University of Edinburgh) for experimental

(39) Content, S.; Kirsch-De Mesmaeker, A. *J. Chem. Soc., Faraday Trans.* **1997**, *93*, 1089−1094.
(40) Holmlin, R. E.; Barton, J. K. *Inorg. Chem.* **1995**, *34*, 7−8.
(41) Mishima, Y.; Motonaka, J.; Ikeda, S. *Anal. Chim. Acta* **1997**, *345*, 45−50.
(42) Dorcier, A.; Dyson, P. J.; Gossens, C.; Rothlisberger, U.; Scopelliti, R.; Tavernelli, I. *Organometallics* **2005**, *24*, 2114−2123.
(43) Binding of $\{(\eta^6\text{-}p\text{-cym})Ru\}^{2+}$ to (deprotonated) $C6NH_2$ of 9-ethyladenine and adenine to N6/7 chelate rings has been observed for a cyclic trimer and tetramer, respectively (Korn, S.; Sheldrick, W. S. *Inorg. Chim. Acta* **1997**, 254, 85−91), but there is no evidence for such binding here.
(44) Lippert, B. *Prog. Inorg. Chem.* **2005**, *54*, 385−447.
(45) Chen, H.; Parkinson, J. A.; Morris, R. E.; Sadler, P. J. *J. Am. Chem. Soc.* **2003**, *125*, 173−186.

assistance, and members of EC COST Group D20 for stimulating discussions.

**Supporting Information Available:** Details of the syntheses and characterization of complexes, crystallographic data, bond lengths and angles (Tables S1, S2), intermolecular interactions and disorder in the X-ray structures of **4**, **4R**, **6**, **7**, and **8** (Figures S1−S3), and NMR studies of hydrolysis and binding to nucleobases (Figures S4−S13); X-ray crystallographic data in CIF format. This material is available free of charge via the Internet at http://pubs.acs.org.

JA055886R